Archives of Mechanics • Archiwum Mechaniki Stosowanej • 27, 3, pp. 417–443, Warszawa 1975

# Large strain, viscoelastic and elasto viscoplastic numerical analysis by means of the finite element method

M. KAWAHARA (TOKYO)

FINITE element procedures and illustrative numerical examples for linear and non-linear viscoelastic and elasto viscoplastic bodies are discussed in this paper. According to the well known theory in rheology, the constitutive equation of viscoelastic body can be described by the first-order simultaneous differential equation system. Using this result, the finite element equation leads to an equation similar to Hookean elastic body except for the inclusion of the time increment. The procedure is applicable to certain forms of non-linear viscoelastic body and elasto viscoplastic body. To solve the non-linear simultaneous equation system, it is convenient to employ the incremental displacement method for non-linear problems such as large deformation loading, unloading and cyclic loading behaviours.

W niniejszej pracy przeprowadzono dyskusję techniki elementów skończonych oraz nieliniowych ciał lepkosprężystych i sprężysto-lepkoplastycznych. Zgodnie z dobrze znaną w reologii teorią równanie konstytutywne dla ciała lepkosprężystego może być opisane równoczesnym układem równań różniczkowych cząstkowych. Korzystając z powyższej własności równanie elementu skończonego jest doprowadzone do równania podobnego do sprężystego ciała Hooka z wyjątkiem uwzględnienia przyrostu czasowego. Procedurę tę stosuje się do pewnych form nieliniowego ciała lepkosprężystego i sprężysto-lepkoplastycznego. Do rozwiązania jednoczesnego nieliniowego układu równań wygodnie jest zastosować metodę przemieszczeń przyrostowych, w szczególności do takich zagadnień nieliniowych jak duże odkształcenia spowodowane obciążeniem, odciążeniem lub obciążeniem cyklicznym.

В настоящей работе проведено обсуждение техники конечных элементов, а также нелинейных вязкоупругих и упруго-вязкопластических тел. Согласно хорошо известной в реологии теории определяющее уравнение для вязкоупругого тела может быть описано совместной системой дифференциальных уравнений в частных производных. Используя вышеприведенные свойства уравнение конечного элемента приведено к уравнению аналогичному упругому телу Гука за исключением учета прироста времени. Эта процедура применяется для некоторых форм нелинейного вязкоупругого и упруго-вязкопластического тела. Для решения совместной нелинейной системы уравнений удобно применять метод перемещений в приростах, в частности для таких нелинейных задач, как большие деформации, вызванные нагрузкой, разгрузкой или циклической нагрузкой.

## 1. Introduction

THE PURPOSE of this paper is to discuss a finite element method for the analysis of viscoelastic and elasto viscoplastic bodies based on both small and large strain theories. In general, viscoelastic body is defined by assuming either generalized strains, i.e., observed strain and hidden strain, or certain forms of Helmholtz free energy. The present paper describes a finite element analysis of viscoelastic body based on the theory of generalized strains and their associated generalized forces. The paper also states that the procedure can be applied to a certain class of non-linear viscoelastic body and elasto viscoplastic body.

According to the concept of generalized strains proposed mainly by BIOT [1] and SCHAPERY [2] the constitutive equation of viscoelastic body can be derived as the first-order simultaneous differential equation system with the relation of Kirchhoff stress, Green strain and hidden strain. Eliminating the hidden strain from this equation system, a higher order differential equation can be obtained relating stress, strain and their time derivatives. The conventional analyses normally use the eliminated equations as the constitutive equations. The concept of the elastic viscoplastic body was developed mainly by PERZYNA [3, 4], after being introduced by HOHENEMSTER and PRAGER [5]. Because the theory is a so-called rate type theory, the procedure for the numerical analysis may be carried out by a method similar to that of the above-mentioned viscoelastic body.

The application of the finite element method to viscoelastic body has been developed and presented by several writers [6–16] under the small displacement assumption. On the basis of large strain theory, ODEN and RAMIRETZ [17] and also ODEN and others [18–22] have discussed finite element methods postulating the functional form for the free energy of the constitutive equation. The author [23–26] has already presented the theoretical basis and several numerical examples for linear and non-linear viscoelastic analysis using the concept of generalized strains. This paper discusses the general numerical procedure of the finite element method on the basis of the constitutive equation involving hidden strain. Taking viscoplastic strain as the hidden strain, the constitutive equation with hidden strain can be regarded as including the elastic viscoplastic body. Thus, the numerical procedures in this paper can also be adopted to the analysis of elastic viscoplastic body.

Replacing the differentiation with respect to time by the difference with respect to short time increment and eliminating the several hidden strains leads to a stress-strain equation similar to elastic body with initial stress components including the time increment in the coefficients. With this stress-strain equation and the fundamental equations of non-linear continuous mechanics, the numerical procedure can be formulated by the following conventional finite element method. The method yields to the non-linear algebraic simultaneous equation system. In order to solve the equation system, the Newton-Raphson method is commonly used. Moreover, the perturbation method is also employed, as it is suitable for adjusting the effects of higher order terms.

## 2. The basic equation

Let $x_i$ and $X_i$ denote spatial and material coordinates, respectively, using the rectangular Cartesian coordinate system with indices $i = 1, 2$ and 3. Indicial notation and summation convention with repeated indices are employed throughout the paper. A subscripted comma $,_i$ means the partial differentiation with respect to $X_i$ and a superposed dot denotes the material time differentiation. It is convenient to take the reference coordinate system $X_i$ and the current coordinate system $x_i$ to coincide in the initial reference state. Then, the relation:

$$x_i = X_i + u_i, \tag{2.1}$$

can be introduced denoting $u_i$ as the components of displacement vector measured along $X_i$ coordinate system. Using the Eq. (2.1), displacement grandient is obtained as:

$$F_{ij} = \chi_{i,j} = \delta_{ij} + u_{i,j}, \tag{2.2}$$

where $\delta_{ij}$ is the Kronecker delta (function). The Green strain tensor $\gamma_{ij}$ is expressed in the form:

$$\gamma_{ij} = \frac{1}{2}(F_{ki}F_{kj} - \delta_{ij}) = \frac{1}{2}(u_{i,j} + u_{j,i} + u_{m,i}u_{m,j}). \tag{2.3}$$

Strain-rate tensor $\dot{\gamma}_{ij}$ is derived by differentiating both sides of the Eq. (2.3) with respect to time;

$$\dot{\gamma}_{ij} = \frac{1}{2}(\dot{u}_{i,j} + \dot{u}_{j,i} + \dot{u}_{m,i}u_{m,j} + u_{m,i}\dot{u}_{m,j}). \tag{2.4}$$

Consider an arbitrary volume $V$ of a continuum surrounded by surface $A$ in the current state, and suppose that $V_0$ is the corresponding volume in the reference state with surface $A_0$. When the surface force $P_i$ is applied across the surface $A$, Kirchhoff stress tensor $S_{ij}$ is introduced as follows:

$$P_i = F_{ij}S_{jk}N_k = S_{jk}(\delta_{ij} + u_{i,j})N_k, \tag{2.5}$$

where $N_k$ are the components of outward unit normal to the surface $A_0$. Using Kirchhoff stress $S_{ij}$, the equilibrium equation is expressed as:

$$(F_{ij}S_{jk})_{,k} + \varrho_0 f_i = 0, \tag{2.6}$$

where $\varrho_0$ is the mass density in the reference state and $f_i$ is the body force. The virtual work equation is introduced from the Eq. (2.6) in order to apply the finite element method. For this purpose boundary conditions of a continuum should be introduced. On the boundary $A_1$, the components of the displacement are prescribed as:

$$u_i = \hat{u}_i \quad \text{on } A_1, \tag{2.7}$$

where $\hat{u}_i$ is the prescribed value of displacement on boundary $A_1$. The surface force $P_i$ applied on boundary $A_2$ is:

$$P_i = \hat{P}_i \quad \text{on } A_2, \tag{2.8}$$

where $P_i$ is the prescribed value on surface $A_2$. It is assumed that

$$A_1 \cup A_2 = A, \tag{2.9}$$

$$A_1 \cap A_2 = \Phi, \tag{2.10}$$

where $\Phi$ is the null set. Multiplying both sides of the Eq. (2.6) by virtual displacement $u_i^*$, which is an arbitrary function except where zero is assumed on boundary $A_1$, and integrating over the whole volume $V_0$, it follows that

$$\int_{V_0} [(F_{ij}S_{jk})_{,k}u_i^*]dV_0 + \int_{V_0} (\varrho_0 f_i u_i^*)dV_0 = 0. \tag{2.11}$$

The application of Green's theorem to the first term of the left-hand side of the Eq. (2.11) leads to the virtual work equation as:

$$\int_{V_0} (S_{ij}\gamma_{ij}^*)dV_0 = \Omega, \tag{2.12}$$

where virtual strain $\gamma_{ij}^*$ is

$$\gamma_{ij}^* = \frac{1}{2}(F_{kj}u_{k,i}^* + F_{k,i}u_{k,j}^*) = \frac{1}{2}(u_{i,j}^* + u_{j,i}^* + u_{m,i}^* u_{m,j} + u_{m,i} u_{m,j}^*), \tag{2.13}$$

and

$$\Omega = \int_{A_0} [S_{ij}N_j(\delta_{ki} + u_{k,i})u_k^*]dA_0 + \int_{V_0} (\varrho_0 f_i u_i^*)dV_0. \tag{2.14}$$

From the Eq. (2.8), the Eq. (2.14) is rewritten as follows:

$$\Omega = \int_{A_2} (\hat{P}_i u_i^*)dA_0 + \int_{V_0} (\varrho_0 f_i u_i^*)dV_0, \tag{2.15}$$

considering $u_i^*$ to be zero on boundary $A_1$.

## 3. Constitutive equations

The basic idea of the constitutive equation employed in this paper was presented by BIOT and SHAPERY. A certain state of the body is assumed to be expressed by generalized strain $q_i$ $(i = 1, 2, \ldots, p)$. Generalized strain consists of observed strain and hidden strain. Green strain $\gamma_{ij}$ is employed as observed strain in this paper. Hidden strain is denoted by $h_{ij}^\alpha$ $(\alpha = 1, 2, \ldots, q)$. Generalized force $Q_i$, corresponding to generalized strain $q_i$, is introduced in such a manner that the product $Q_i\dot{q}_i$ would be equivalent to the work $S_{ij}\dot{\gamma}_{ij}$. Namely, the part of $Q_i$ corresponding to observed strain is Kirchhoff stress $S_{ij}$ and the part corresponding to hidden strain is taken to be zero. Assumptions are made on the generalized force that it consists of a reversible part $Q_i^{(R)}$ and an irreversible part $Q_i^{(I)}$ and, moreover, $Q_i^{(R)}$ and $Q_i^{(I)}$ are given by linear functions of generalized strain $q_i$ and its time rate $\dot{q}_i$, respectively.

Based on the above assumptions, the constitutive equation of the viscoelastic body can be expressed in the following form:

$$Q_i = a_{ij}q_j + b_{ij}\dot{q}_j, \tag{3.1}$$

where $a_{ij}$ and $b_{ij}$ are positive semi-definite constant arrays. If $q_1$ through $q_6$ are taken to be strain $\gamma_{ij}$, then $Q_1$ through $Q_6$ will be stress $S_{ij}$. Taking this into account, the Eq. (3.1) is rewritten into two systems of equations as follows:

$$S_{ij} = A_{ijkl}^{(1)}\gamma_{kl} + A_{ijkl\alpha}^{(2)}h_{kl}^\alpha + B_{ijkl}^{(1)}\dot{\gamma}_{kl} + B_{ijkl\alpha}^{(2)}\dot{h}_{kl}^\alpha, \tag{3.2}$$

$$A_{ijkl\alpha}^{(2)}\gamma_{ij} + A_{ijkl\alpha\beta}^{(3)}h_{ij}^\beta + B_{ijkl\alpha}^{(2)}\dot{\gamma}_{ij} + B_{ijkl\alpha\beta}^{(3)}\dot{h}_{ij}^\beta = 0. \tag{3.3}$$

For brevity, the constitutive equations (3.2) and (3.3) are expressed in the form:

$$Q_{ij}^\alpha = A_{ijkl}^{\alpha\beta}h_{kl}^\beta + B_{ijkl}^{\alpha\beta}\dot{h}_{kl}^\beta, \quad i, j, k, l = 1, 2, 3;\ \alpha, \beta = 1, 2, \ldots, q, \tag{3.4}$$

where

$$Q_{ij}^1 = S_{ij}, \quad h_{ij}^1 = \gamma_{ij} \quad \text{and} \quad Q_{ij}^\beta = 0\ (\beta \neq 0). \tag{3.5}$$

The constant arrays $A_{ijkl}^{\alpha\beta}$ and $B_{ijkl}^{\alpha\beta}$ can be obtained by formulating in accordance with the so-called rheological model. Consider an arbitrary rheological model as shown in

Fig. 1. The rheological element of the model is both spring element $E^{mn}_{ijkl}$ and dashpot element $C^{mn}_{ijkl}$. Numbering arbitrarily the nodes of the model to which the elements are connected and regarding the generalized strain $h^{\alpha}_{ij}$ to correspond to each model, the

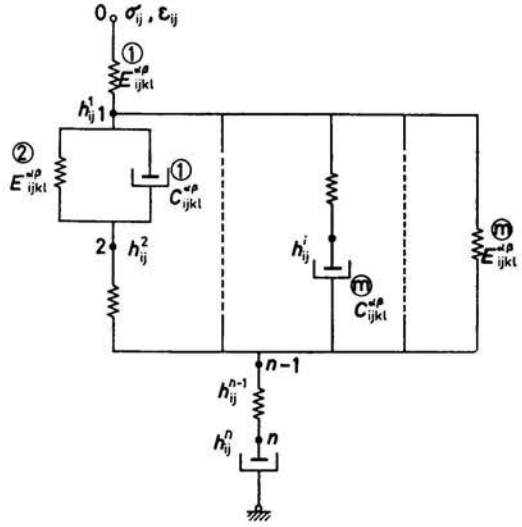


FIG. 1. Rheological model.

following procedure for $A^{\alpha\beta}_{ijkl}$ and $B^{\alpha\beta}_{ijkl}$ can be obtained. Namely, if the $m$th spring element $E^m_{ijkl}$ (or $n$th dashpot element $C^n_{ijkl}$) is connected to the nodes $\lambda$ and $\mu$, then the array $A^{\alpha\beta}_{ijkl}$ (or $B^{\alpha\beta}_{ijkl}$) can be constructed by algorithm

$$
\begin{aligned}
&A^{\lambda\lambda}_{ijkl} = A^{\lambda\lambda}_{ijkl} + E^m_{ijkl}, && B^{\lambda\lambda}_{ijkl} = B^{\lambda\lambda}_{ijkl} + C^n_{ijkl},\\
&A^{\lambda\mu}_{ijkl} = A^{\mu\lambda}_{ijkl} = -E^m_{ijkl}, && B^{\lambda\mu}_{ijkl} = B^{\mu\lambda}_{ijkl} = -C^n_{ijkl},\\
&A^{\mu\mu}_{ijkl} = A^{\mu\mu}_{ijkl} + E^m_{ijkl}, && B^{\mu\mu}_{ijkl} = B^{\mu\mu}_{ijkl} + C^n_{ijkl},
\end{aligned}
\tag{3.6}
$$

in which the range of index $m$ (or $n$) is from 1 to $r$ (or $s$) where $r$ (or $s$) is the total number of spring (or dashpot) elements of the model.

In the conventional analysis of viscoelastic body, the higher order differential equation is often employed involving only stress, strain and their time rate. This equation is obtained by eliminating hidden strain $h^{\alpha}_{ij}$ from the Eq. (3.2) using the Eq. (3.3). From the computational point of view, it is more convenient to use the Eq. (3.4) directly than to use the above-mentioned eliminated equation because of its simplicity and because its system is suitable for the application of the finite element method. The Eq. (3.4) is the first-order differential equation. The right-hand side of the Eq. (3.4) does not involve stress and stress rate implicitly. The former statement is important because it is easier to handle the first-order simultaneous differential equation in the case of computation by digital computers. The latter statement implies that the constitutive equation (3.4) is suitable for the application of the displacement method, which is one of the main procedures of the finite element method.

## 4. The finite element method

Consider a short time increment $\Delta t$, and suppose that $\dot{h}^{\beta}_{ij}$ can be regarded to be constant during this increment, i.e.,

$$\dot{h}^{\beta}_{ij} = (h^{\beta}_{ij} - h^{\beta}_{ij}(0))/\Delta t, \tag{4.1}$$

where $h^{\beta}_{ij}$ and $h^{\beta}_{ij}(0)$ mean the final and initial value of the time increment $\Delta t$, respectively. Using the Eq. (4.1), the Eq. (3.4) is transformed into the following form:

$$Q^{\alpha}_{ij} = K^{\alpha\beta}_{ijkl} h^{\beta}_{kl} + H^{\alpha\beta}_{ijkl} h^{\beta}_{kl}(0), \tag{4.2}$$

where

$$K^{\alpha\beta}_{ijkl} = A^{\alpha\beta}_{ijkl} + \frac{1}{\Delta t} B^{\alpha\beta}_{ijkl}, \qquad H^{\alpha\beta}_{ijkl} = -\frac{1}{\Delta t} B^{\alpha\beta}_{ijkl},$$

which is resolved into two systems of equations taking the Eq. (3.5) into account;

$$S_{ij} = K^{(1)}_{ijkl}\gamma_{kl} + K^{(2)}_{ijkl\alpha} h^{\alpha}_{kl} + H^{(1)}_{ijkl}\gamma_{kl}(0) + H^{(2)}_{ijkl\alpha} h^{\alpha}_{kl}(0), \tag{4.3}$$

$$K^{(2)}_{ijkl\alpha}\gamma_{ij} + K^{(3)}_{ijkl\alpha\beta} h^{\beta}_{ij} + H^{(2)}_{ijkl\alpha}\gamma_{ij}(0) + H^{(3)}_{ijkl\alpha\beta} h^{\beta}_{ij}(0) = 0. \tag{4.4}$$

From the Eq. (4.3) and (4.4), the stress-strain relation of the viscoelastic body can be expressed by an equation similar to Hookean body as follows:

$$S_{ij} = D_{ijkl}\gamma_{kl} + \bar{S}_{ij}, \tag{4.5}$$

$$h^{\alpha}_{ij} = -S^{(1)}_{\alpha}\gamma_{ij} - S^{(2)}_{\alpha}\gamma_{ij}(0) - S^{(3)}_{\alpha\beta} h^{\beta}_{ij}(0), \tag{4.6}$$

where

$$S^{(1)}_{\alpha} = L^{(3)}_{ijkl\alpha\gamma} K^{(2)}_{ijkl\gamma}, \quad S^{(2)}_{\alpha} = L^{(3)}_{ijkl\alpha\gamma} H^{(2)}_{ijkl\gamma}, \quad S^{(3)}_{\alpha\beta} = L^{(3)}_{ijkl\alpha\gamma} H^{(3)}_{ijkl\gamma\beta},$$

$$K^{(3)}_{ijkl\alpha\beta} L^{(3)}_{mnpq\gamma\delta} = \delta_{im}\delta_{jn}\delta_{kp}\delta_{lq}\delta_{\alpha\gamma}\delta_{\beta\delta},$$

$$D_{ijkl} = K^{(1)}_{ijkl} - K^{(2)}_{ijmn\gamma} L^{(3)}_{mnpq\gamma\delta} K^{(2)}_{pqkl\delta},$$

$$\bar{S}_{ij} = (H^{(1)}_{ijkl} - K^{(2)}_{ijkl\beta} S^{(2)}_{\beta})\gamma^{(0)}_{kl} + (H^{(2)}_{ijkl\gamma} - K^{(2)}_{ijkl\beta} S^{(3)}_{\beta\gamma}) h^{\gamma}_{kl}(0).$$

According to the conventional finite element procedure, a continuous medium should be divided into small regions called finite elements. The displacement of $\alpha$th node in the $i$th direction is denoted by $u_{\alpha i}$ on each finite element. The displacement inside the finite element is assumed to be approximated with the aid of the shape function $\Phi_{\alpha}$ as follows:

$$u_i = \Phi_{\alpha} u_{\alpha i}; \tag{4.7}$$

substituting this into the Eq. (2.3) and the Eq. (2.13), $\gamma_{ij}$ and $\gamma^{*}_{ij}$ are expressed as:

$$2\gamma_{ij} = \Phi_{\alpha,i} u_{\alpha j} + \Phi_{\alpha,j} u_{\alpha i} + \Phi_{\alpha,i}\Phi_{\beta,j} u_{\alpha k} u_{\beta k}, \tag{4.8}$$

and

$$2\gamma^{*}_{ij} = \Phi_{\alpha,i} u^{*}_{\alpha j} + \Phi_{\alpha,j} u^{*}_{\alpha i} + \Phi_{\alpha,i}\Phi_{\beta,j} u^{*}_{\alpha k} u_{\beta k} + \Phi_{\alpha,i}\Phi_{\beta,j} u_{\alpha k} u^{*}_{\beta k}. \tag{4.9}$$

Introducing the Eq. (4.5) into the Eq. (2.12), it follows that

$$\int_{V_0} (D_{ijkl}\gamma_{ij}\gamma^{*}_{kl})\, dV_0 + \int_{V_0} (\bar{S}_{ij}\gamma^{*}_{ij})\, dV_0 = \Omega. \tag{4.10}$$

Substitution of the Eqs. (4.7), (4.8) and (4.9) into the Eq. (4.10), rearrangement of the resulting equation and the use of the arbitrariness of the virtual displacement $u^*_{\alpha i}$ leads to the finite element formulation

$$K_{\alpha i \beta j} u_{\beta j} = \Omega_{\alpha i} - \bar{\Omega}_{\alpha i}, \tag{4.11}$$

where

$$K_{\alpha i \beta j} = \int_{V_0} \left[ \Phi_{\alpha,k} (\delta_{li} + \Phi_{\delta,l} u_{\delta i}) D_{klmn} \left( \delta_{mj} + \frac{1}{2} \Phi_{\gamma,m} u_{\gamma j} \right) \Phi_{\beta n} \right] dV_0, \tag{4.12}$$

$$\Omega_{\alpha i} = \int_{A_2} (p_i \Phi_\alpha) dA_0 + \int_{V_0} (\varrho_0 f_i \Phi_\alpha) dV_0, \tag{4.13}$$

$$\bar{\Omega}_{\alpha i} = \int_{V_0} [\bar{S}_{kl} (\delta_{li} + \Phi_{\delta,l} u_{\delta i}) \Phi_{\alpha,k}] dV_0. \tag{4.14}$$

The term $K_{\alpha i \beta j}$ in the left-hand side of the Eq. (4.11) corresponds to the stiffness matrix in the conventional finite element method and is related to the viscoelastic modulus and short time increment $\Delta t$. The term $\Omega_{\alpha i} - \bar{\Omega}_{\alpha i}$ is the equivalent load term and $\bar{\Omega}_{\alpha i}$ expresses the influence of the history of deformation.

## 5. Solution procedures

For each time increment $\Delta t$, the simultaneous equation system on the whole continuum can be formulated by following the conventional finite element method and is expressed as follows:

$$F_N = \Psi_N(u_M) - \Omega_N = 0, \tag{5.1}$$

where $u_M$ are the displacements of all the nodal points of the continuum, $\Psi_N(u_M)$ is the non-linear function resulting from the left-hand side of the Eq. (4.11) and $\Omega_N$ is the prescribed function from the right-hand side of the Eq. (4.11). For the solution procedure of the non-linear simultaneous equation system, the Newton-Raphson method is commonly used. The procedure is expressed as follows:

$$u_N^{(i)} = u_N^{(i-1)} - \left[ \frac{\partial F_N^{(i-1)}}{\partial u_M} \right]^{-1} F_M^{(i-1)}, \tag{5.2}$$

where $(i)$ represents $i$th iteration cycle of the procedure and $\left[ \frac{\partial F_N}{\partial u_M} \right]$ is the gradient of $F_N$, which is easily calculated using the Eqs. (5.1) and (4.11).

To solve the non-linear simultaneous equation (5.1), the perturbation method is also utilized in this paper. The method involves the calculation to proceed step by step applying the increments of external load or prescribed displacement. The former method is called the incremental displacement method. Let the term be expanded into the following expression:

$$\Omega_N = \Omega_N^{(0)} + \varepsilon \Omega_N^{(1)} + \frac{1}{2} \varepsilon^2 \Omega_N^{(2)} + \ldots \tag{5.3}$$

where $\varepsilon$ is the given small parameter. By expanding the displacement $u_M$ as:

$$u_M = u_M^{(0)} + \varepsilon u_M^{(1)} + \frac{1}{2}\varepsilon^2 u_M^{(2)} + \ldots, \tag{5.4}$$

introducing the Eqs. (5.3) and (5.4) into the Eq. (5.1), and comparing the terms of the same order of $\varepsilon$, the following linear simultaneous equation system is obtained

$$\begin{aligned} \overline{\Psi}_N^{(0)}(u_M^{(0)}) - \Omega_N^{(0)} &= 0, \\ \overline{\Psi}_N^{(1)}(u_M^{(0)})u_M^{(1)} - \Omega_N^{(1)} &= 0, \\ \overline{\Psi}_N^{(2)}(u_M^{(0)}, u_M^{(1)})u_M^{(2)} - \Omega_N^{(2)} &= 0, \\ &\cdots\cdots\cdots\cdots\cdots \end{aligned} \tag{5.5}$$

The equation (5.5) with the unknown $u_M^{(i)}$ can be solved provided the solutions up to the $(i-1)$th order are all known. This procedure is called the incremental loading method or the incremental displacement method as $\Omega_N$ is calculated from the external applied load or the prescribed boundary displacement.

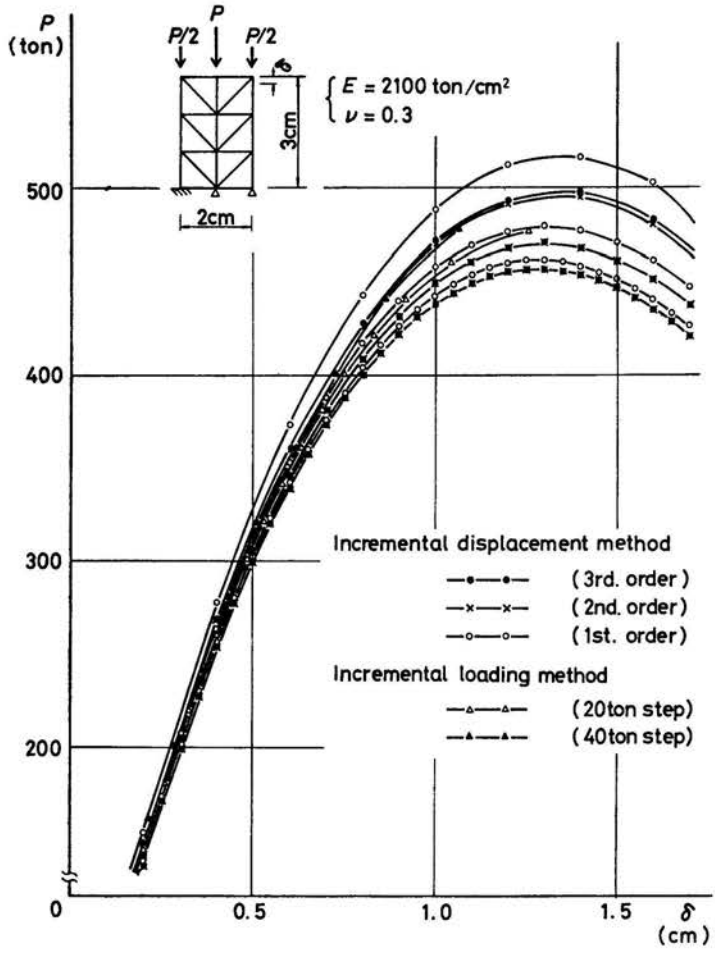


FIG. 2. Load displacement diagram of Hookean elastic body.

Figure 2 shows the calculated load displacement diagram assuming Hookean elastic stress-strain relation between Green strain and Kirchhoff stress. Comparative results obtained by the incremental loading method and the incremental displacement method are illustrated. Truncated errors by the incremental displacement method are also compared numerically. From these results, if the increments of the prescribed displacement are taken to be small enough, as illustrated in the figure, then the difference of the truncation up to the third-order and second-order can be regarded as negligibly small.

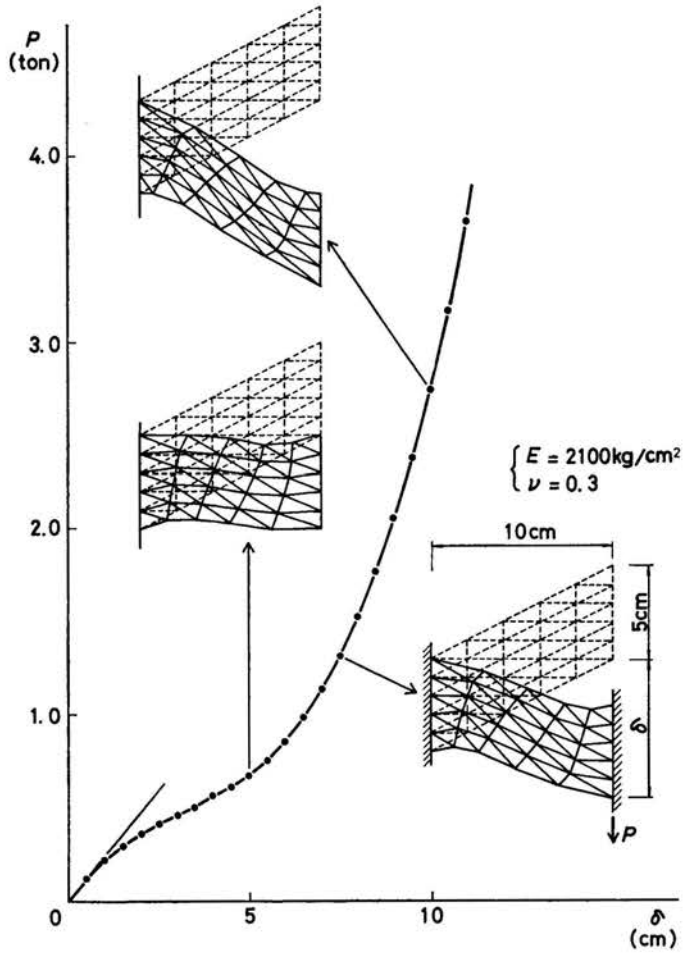


FIG. 3. Load displacement diagram and deformation shapes.

Figure 3 shows the calculated load displacement diagram and the deformed shapes of cantilever beam calculated by the incremental displacement method. These figures indicate that it is more appropriate to compute the unloading behaviour or the comparatively large deformation behaviour by the incremental displacement method than by the incremental loading method.

## 6. Small strain non-linear creep analysis of beam

In order to illustrate the procedure, non-linear creep analysis of a three-bar truss and cantilever beam is performed. The following constitutive equation is often employed to express non-linear creep in one-dimensional case:

$$\dot{\varepsilon} = \frac{\dot{\sigma}}{E} + \frac{1}{\lambda}\left(\frac{\sigma}{\sigma^*}\right)^n. \tag{6.1}$$

The Eq. (6.1) is rewritten in the following form using hidden strain $h$

$$\begin{bmatrix} \sigma \\ \hline 0 \end{bmatrix} = \left[\begin{array}{c|c} E & -E \\ \hline -E & E \end{array}\right] \begin{bmatrix} \varepsilon \\ \hline h \end{bmatrix} + \left[\begin{array}{c|c} 0 & 0 \\ \hline 0 & \lambda\sigma^*\left(\frac{\sigma}{\sigma^*}\right)^{1-n} \end{array}\right] \begin{bmatrix} \dot{\varepsilon} \\ \hline \dot{h} \end{bmatrix}, \tag{6.2}$$

in which $E$, $\lambda$ and $\sigma^*$ are the viscoelastic constants. The Eq. (6.2) expresses a similar relation to the Eq. (3.4). Accordingly, the same procedures as described in the previous section can be applied to the analysis.

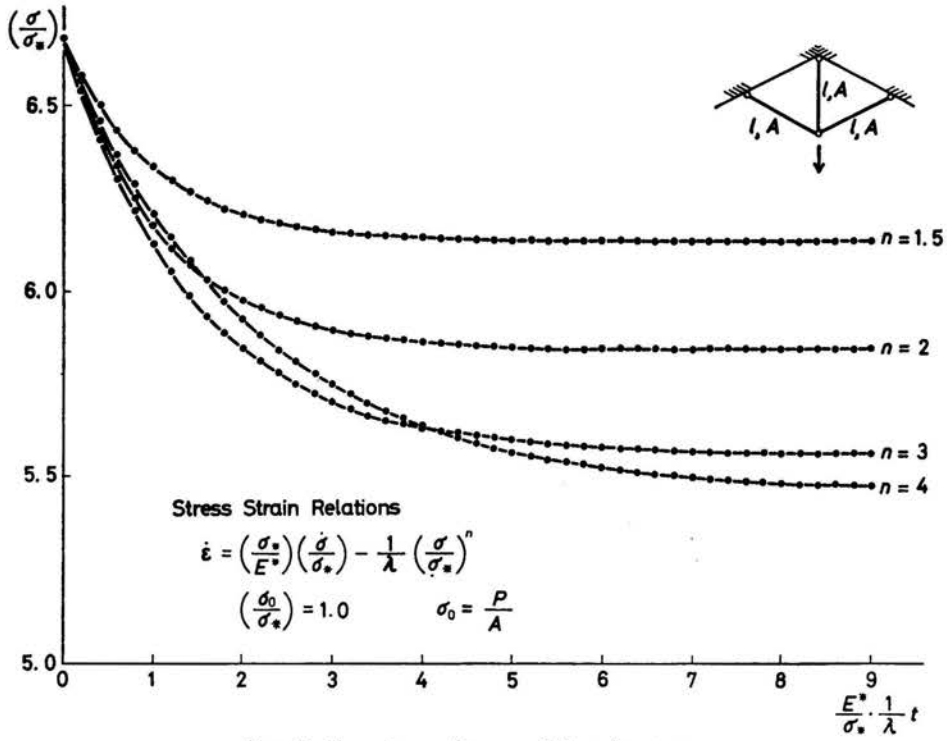


FIG. 4. Time stress diagram of three-bar truss.

Figure 4 shows the stress changes in the middle member of a three-bar truss for the various exponents $n$. The time stress relation of a cantilever beam is calculated in Fig. 5. In the case of a cantilever beam, the stress distribution within one element differs across the section of the beam. Therefore, the finite element is subdivided into smaller sub-

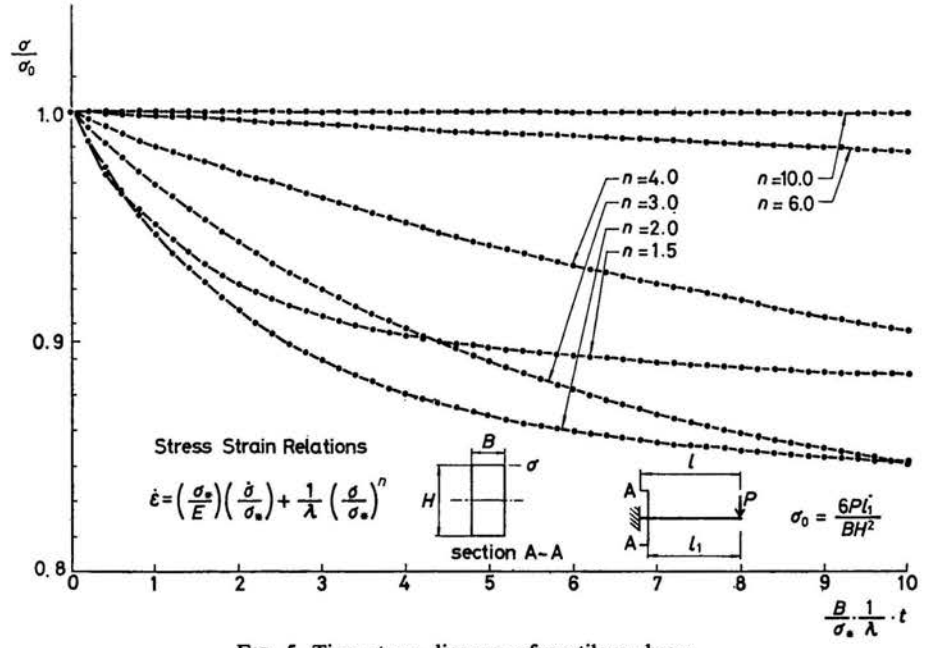


FIG. 5. Time stress diagram of cantilever beam.

elements for the calculation of stress and integral evaluation. Figure 6 shows the stress distribution in section as compared with the analytical solution. The conventional shape functions are used, i.e., linear for truss analysis and the third-order for cantilever beam analysis, assuming small deformation.

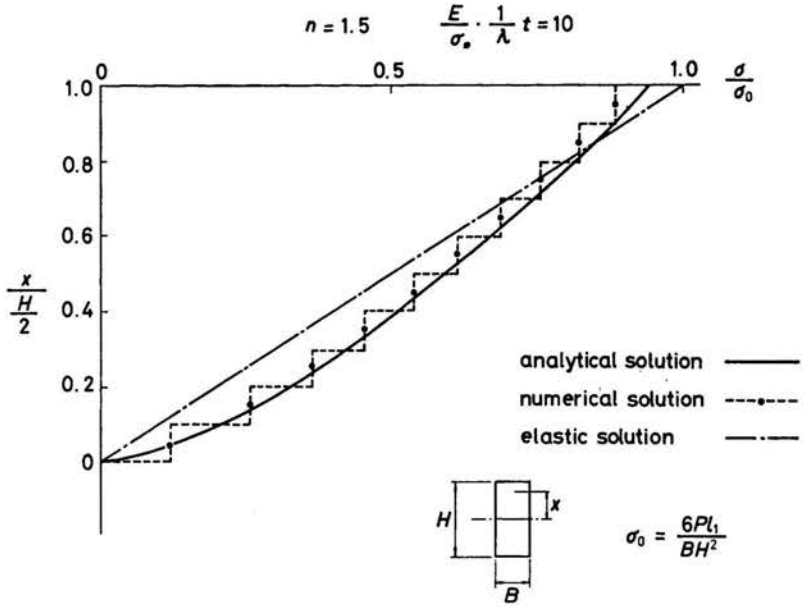


FIG. 6. Stress distribution of section A-A.

## 7. Large strain, creep and relaxation analysis

The constitutive equation formulated by a three-element model as shown in Fig. 7 is a commonly used rheological equation to express creep and relaxation behaviour of a continuum. In the analysis shown in Figs. 7 and 8, the volumetric components of stress

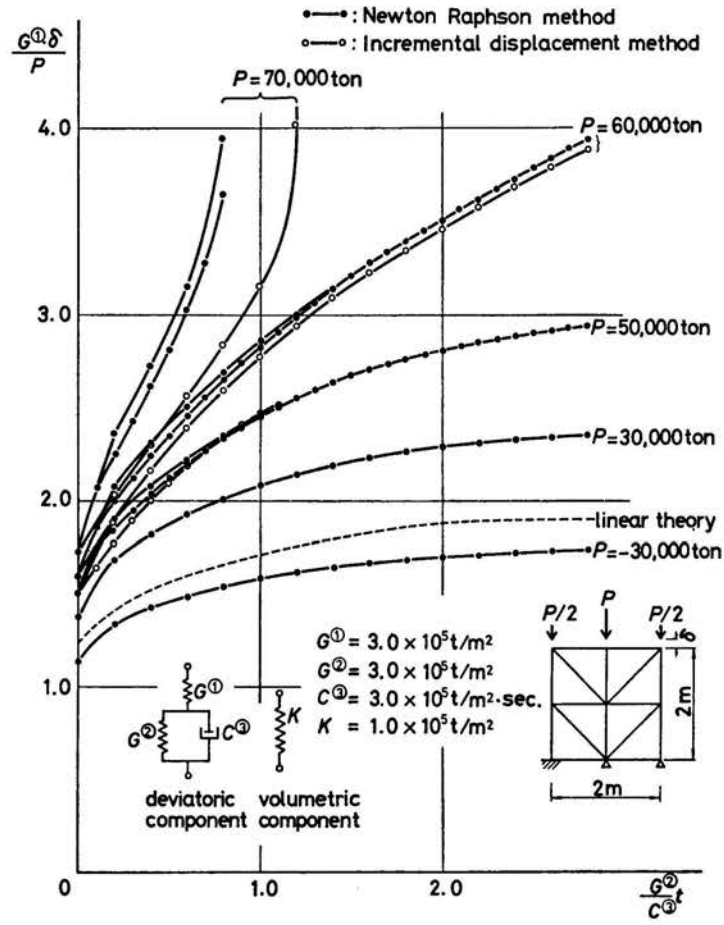


FIG. 7. Time displacement diagram (creep curve).

and strain are considered to respond as an elastic body expressed by the three-element model. Following the algorithm of the Eq. (3.6), the constitutive equation is expressed as follows:

$$\left[\begin{array}{c}\tau_{ij}\\ \hline 0\end{array}\right]=\left[\begin{array}{c|c}2G^{(1)} & -2G^{(1)}\\ \hline -2G^{(1)} & 2(G^{(1)}+G^{(2)})\end{array}\right]\left[\begin{array}{c}e_{ij}\\ \hline h_{ij}\end{array}\right]+\left[\begin{array}{c|c}0 & 0\\ \hline 0 & 2C^{(3)}\end{array}\right]\left[\begin{array}{c}\dot{e}_{ij}\\ \hline \dot{h}_{ij}\end{array}\right], \tag{7.1}$$

$$S_{kk}=3K\gamma_{kk}, \tag{7.2}$$

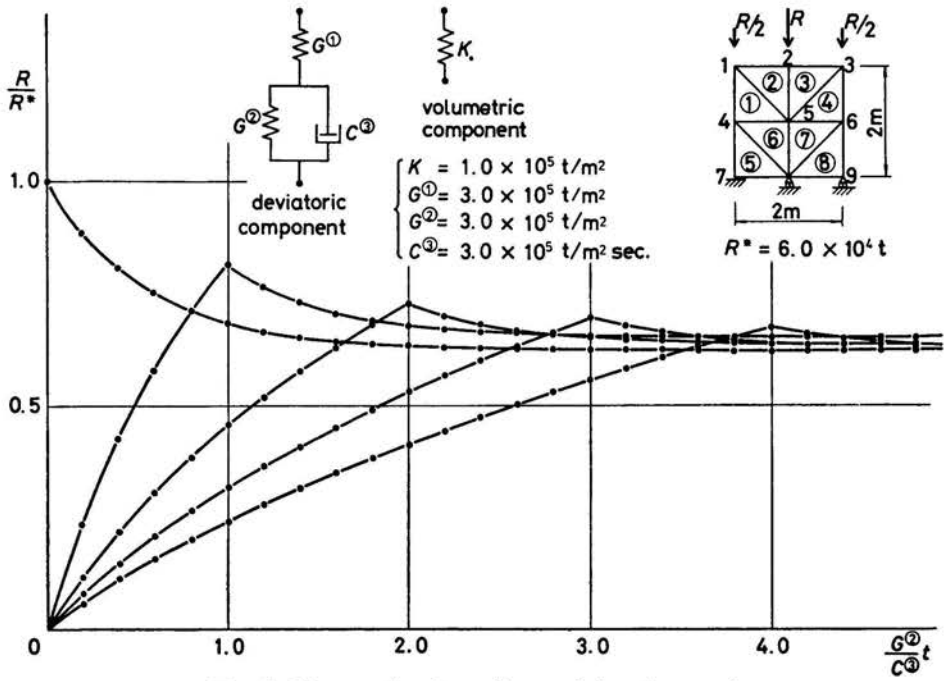


FIG. 8. Time reaction force diagram (relaxation curve).

where $\tau_{ij}$ and $e_{ij}$ denote deviatoric stress and strain, respectively, and they are expressed in the following forms:

$$\tau_{ij} = S_{ij} - \frac{S_{kk}}{3}\delta_{ij}, \tag{7.3}$$

$$e_{ij} = \gamma_{ij} - \frac{\gamma_{kk}}{3}\delta_{ij}. \tag{7.4}$$

In the Eqs. (7.1) and (7.2), quantities $G^{(1)}$, $G^{(2)}$, $C^{(3)}$ and $K$ are the viscoelastic constants as shown in Fig. 7 and $h_{ij}$ is the hidden strain. Corresponding to the Eqs. (4.5) and (4.6), the following equations (7.5) and (7.6) are derived from the Eqs. (7.1) and (7.2),

$$\tau_{ij} = 2G^{(1)}\left(1 - \frac{G^{(1)}}{G^{(1)}+G^{(2)}+C^{(3)}/\Delta t}\right)e_{ij} + 2G^{(1)}\frac{C^{(3)}/\Delta t}{G^{(1)}+G^{(2)}+C^{(3)}/\Delta t}h_{ij}(0), \tag{7.5}$$

$$h_{ij} = \frac{G^{(1)}}{G^{(1)}+G^{(2)}+C^{(3)}/\Delta t}e_{ij} + \frac{C^{(3)}/\Delta t}{G^{(1)}+G^{(2)}+C^{(3)}/\Delta t}h_{ij}(0). \tag{7.6}$$

Employing a triangular finite element and a constant strain type shape function with area coordinate, the computation, of which numerical results are shown in Figs. 7 and 8, is carried out using the Eq. (4.11) with the Eqs. (7.5) and (7.6).

In order to illustrate the procedure, a simple numerical example in Fig. 7 is treated, which is the calculation of the tertiary creep as well as the secondary and initial creep. In Fig. 7, calculated results obtained by the Newton-Raphson method and the incremental displacement method are plotted comparatively. When the values of the external load

do not exceed 60.000$^t$, the calculated results by both methods are well in agreement. However, when the external load reaches up to 70.000$^t$, the calculated displacements by both methods show a discrepancy. In view of this, the difference seems to come from the numerical procedure, especially from the difference of the transformed relation of the constitutive equation. In the procedure of the Newton-Raphson method, the Eqs. (7.5) and (7.6) are employed. For the incremental displacement method, introducing the second part of the Eq. (7.1) into the first part of the Eq. (7.1), the following is obtained:

$$\tau_{ij} = 2G^{(1)}(e_{ij}-h_{ij}), \tag{7.7}$$

$$\tau_{ij}+2G^{(2)}h_{ij}+2C^{(3)}\dot{h}_{ij} = 0. \tag{7.8}$$

Differentiating both sides of the Eq. (7.7) with respect to time $t$ and eliminating $\dot{h}_{ij}$ from the resulting equation using the Eq. (7.8), the following equation is obtained:

$$\dot{\tau}_{ij} = 2G^{(1)}\dot{e}_{ij}-\frac{G^{(1)}}{C^{(3)}}\tau_{ij}-\frac{2G^{(1)}G^{(2)}}{C^{(3)}}h_{ij}. \tag{7.9}$$

From the Eqs. (7.2) and (7.9), it follows that

$$\dot{S}_{ij} = \{\mu(\delta_{ik}\delta_{jl}+\delta_{il}\delta_{jk})+\lambda\delta_{ij}\delta_{kl}\}\dot{\gamma}_{kl}+k_1 S_{ij}+k_2 h_{ij}, \tag{7.10}$$

where

$$\mu = G^{(1)}, \qquad k_1 = -\frac{G^{(1)}}{C^{(3)}},$$

$$\lambda = \frac{3K-2G^{(1)}}{3}, \qquad k_2 = \frac{2G^{(1)}G^{(2)}}{C^{(3)}}.$$

By expanding $S_{ij}$, $\gamma_{ij}$ and $h_{ij}$ into Taylor's series as:

$$S_{ij} = S_{ij}^{(0)}+S_{ij}^{(1)}\Delta t+\frac{1}{2}S_{ij}^{(2)}\Delta t^2+\ldots, \tag{7.11}$$

$$\gamma_{ij} = \gamma_{ij}^{(0)}+\gamma_{ij}^{(1)}\Delta t+\frac{1}{2}\gamma_{ij}^{(2)}\Delta t^2+\ldots, \tag{7.12}$$

$$h_{ij} = h_{ij}^{(0)}+h_{ij}^{(1)}\Delta t+\frac{1}{2}h_{ij}^{(2)}\Delta t^2+\ldots, \tag{7.13}$$

introducing the Eqs. (7.11) to (7.13) into the Eq. (7.10) and rearranging them, $S_{ij}^{(n)}$ is obtained as

$$S_{ij}^{(n)} = E_{ijkl}\gamma_{kl}^{(n)}+k_1 S_{ij}^{(n-1)}+k_2 h_{ij}^{(n-1)}, \tag{7.14}$$

for the $n$th order term of $\Delta t$. Using the Eq. (7.14), a finite element governing equation concerning the first two order terms is obtained.

For the first-order term:

$$\bar{K}_{\alpha i\beta j}\cdot u_{\beta i}^{(1)} = \Omega_{\alpha i}^{(1)}-\bar{\Omega}_{\alpha i}^{(0)}. \tag{7.15}$$

For the second-order term:

$$\bar{K}_{\alpha i\beta j}u_{\beta j}^{(2)} = \Omega_{\alpha i}^{(2)}-\hat{\Omega}_{\alpha i}^{(2)}-\bar{\Omega}_{\alpha i}^{(1)}, \tag{7.16}$$

where

$$\overline{K}_{\alpha i\beta j} = \int_{V_0} [\Phi_{\alpha,k}(\delta_{il}+\Phi_{\delta,l}u_{\delta i}^{(0)})E_{klmn}(\delta_{mj}+\Phi_{\gamma,m}u_{\gamma j}^{(0)})\Phi_{\beta,n}+\Phi_{\alpha,k}\delta_{ij}S_{kl}^{(0)}\Phi_{\beta,l}]dV_0,$$

$$\overline{\Omega}_{\alpha i}^{(i)} = \int_{V_0} [\Phi_{\alpha,k}(\delta_{il}+\Phi_{\beta,l}u_{\beta i}^{(0)})H_{kl}^{(i)}]dV_0,$$

$$H_{kl}^{(i)} = k_1 S_{kl}^{(i-1)}+k_2 h_{kl}^{(i-1)},$$

$$\hat{\Omega}_{\alpha i}^{(2)} = \int_{V_0} [\Phi_{\alpha,k}(\delta_{il}+\Phi_{\beta,l}u_{\beta i}^{(0)})E_{klmn}\Phi_{\gamma,m}\Phi_{\delta,n}u_{\gamma r}^{(1)}u_{\delta r}^{(1)}+2\Phi_{\alpha,k}\Phi_{\beta,l}u_{\beta i}^{(1)}S_{kl}^{(1)}]dV_0.$$

Figure 8 is an illustrative example of a relaxation behaviour of viscoelastic body calculated by the incremental displacement method. Figure 8 shows the time reaction force diagram, which is calculated in the following manner. Up to a certain time, the prescribed displacement of the nodal point 1, 2 and 3 is made to increase by steps, and then to keep the displacements fixed at the constant values.

## 8. Elasto viscoplastic analysis by Newton-Raphson method

Introducing deviatoric stress $\tau_{ij}$ and strain $e_{ij}$ as in the Eqs. (7.3) and (7.4), it is assumed that strain $e_{ij}$ is decomposed into the sum of elastic strain $e_{ij}^{(e)}$ and viscoplastic strain $e_{ij}^{(p)}$ as:

$$e_{ij} = e_{ij}^{(e)}+e_{ij}^{(p)}. \tag{8.1}$$

Hookean elastic law is assumed to be valid for elastic strain $e_{ij}^{(e)}$ and $\gamma_{ii}^{(e)}$;

$$\tau_{ij} = 2Ge_{ij}^{(e)} = 2G(e_{ij}-e_{ij}^{(p)}), \tag{8.2}$$

$$S_{ii} = 3K\gamma_{ii}^{(e)}, \tag{8.3}$$

where $G$ and $K$ are shear and volumetric modulus, respectively. In the viscoplastic body introduced by PERZYNA, its viscoplastic strain $e_{ij}^{(p)}$ can be expressed in the following form:

$$\dot{\gamma}_{ij}^{(p)} = \frac{k}{\eta}\gamma_0\langle\Phi(F)\rangle\frac{\partial F}{\partial\tau_{ij}}, \tag{8.4}$$

where $k$, $\eta$ and $\gamma_0$ are constants, $F$ is the yielding function and the notation $\langle\ \rangle$ means:

$$\langle\Phi(F)\rangle = \begin{cases} 0 & \text{if} \quad F\leqslant 0, \\ \Phi(F) & \text{if} \quad F>0. \end{cases} \tag{8.5}$$

For the yielding function $F$, the following von Mises type function is employed:

$$F = \frac{J_2^{1/2}}{k}-1 = \frac{1}{k}(\tau_{ij}\tau_{ij})^{1/2}-1. \tag{8.6}$$

In the Eq. (8.9), $J_2^{1/2}$ is the second invariant of deviatoric stress $\tau_{ij}$. The constant $k$ denotes the shear strength of the material. For the function $\Phi(F)$, the following is introduced:

$$\Phi(F) = F^{\delta} = \left(\frac{J_2^{1/2}}{k}-1\right)^{\delta}. \tag{8.7}$$

Using the Eqs. (8.1) to (8.7), the constitutive equations of the elasto viscoplastic body employed in the present analysis are arranged in the following forms:

For the elastic region ($J_2^{1/2} \leqslant k$):

$$\tau_{ij} = 2Ge_{ij}, \quad S_{kk} = 3K\gamma_{kk}. \tag{8.8}$$

For the viscoplastic region ($J_2^{1/2} > k$):

$$\tau_{ij} = 2G(e_{ij} - e_{ij}^{(p)}), \quad S_{kk} = 3K\gamma_{kk}, \tag{8.9}$$

$$\dot{e}_{ij} = \gamma\left(\frac{J_2^{1/2}}{k} - 1\right)^{\delta} \frac{\tau_{ij}}{J_2^{1/2}} \equiv \frac{1}{\pi}\tau_{ij},$$

where $\gamma = \dfrac{\gamma_0}{2k}$.

The Eq. (8.9) can be rewritten in a similar form to the Eq. (3.4) under the same procedure as that of the Eq. (6.1) to the Eq. (6.2). However, in this case it seems more convenient to proceed with the analysis by the direct use of the Eq. (8.9).

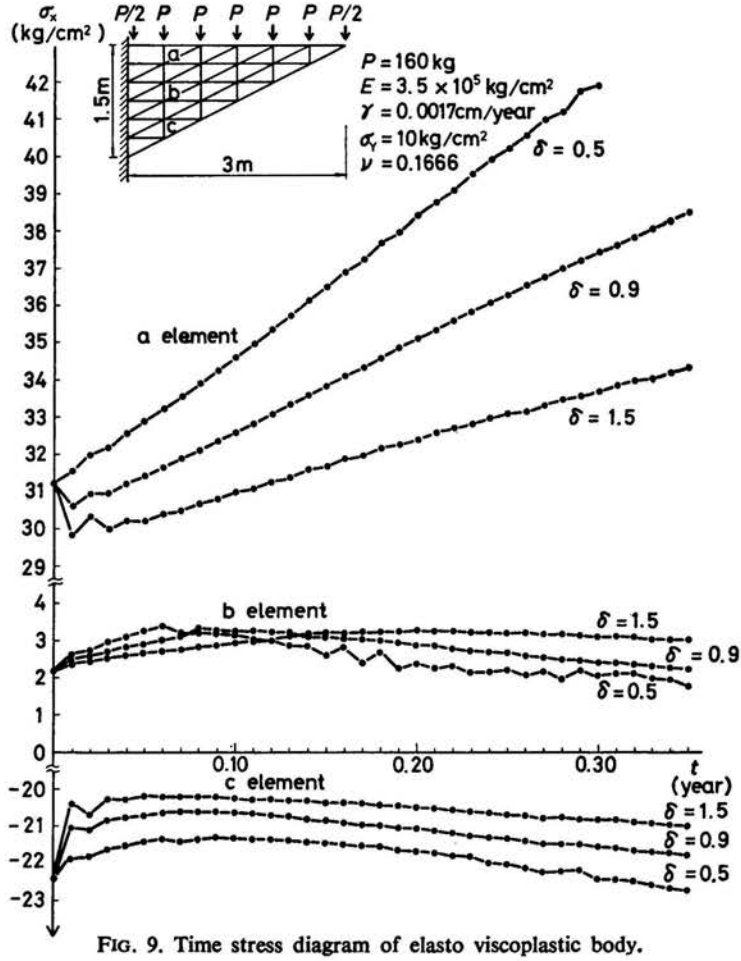


FIG. 9. Time stress diagram of elasto viscoplastic body.

Assuming that the differentiation with respect to time $t$ is replaced by the difference with respect to time increment $\Delta t$, then

$$\dot{e}_{ij}^{(p)} = \frac{e_{ij}^{(p)} - e_{ij}^{(p)}(0)}{\Delta t}, \tag{8.10}$$

where $e_{ij}^{(p)}$ and $e_{ij}^{(p)}(0)$ represent the final and initial value of the viscoplastic strain in the short time increment $\Delta t$, respectively. Substitution of the Eq. (8.10) into the Eq. (8.9) and the rearrangement of the terms yields the following equation:

$$\tau_{ij} = 2\mu^* e_{ij}^{(p)} - H_{ij}, \tag{8.11}$$

where

$$\mu^* = G\left(1 - \frac{2G}{\frac{\pi}{\Delta t} + 2G}\right), \qquad H_{ij} = \frac{2G\frac{\pi}{\Delta t}}{\frac{\pi}{\Delta t} + 2G} e_{ij}^{(p)}(0).$$

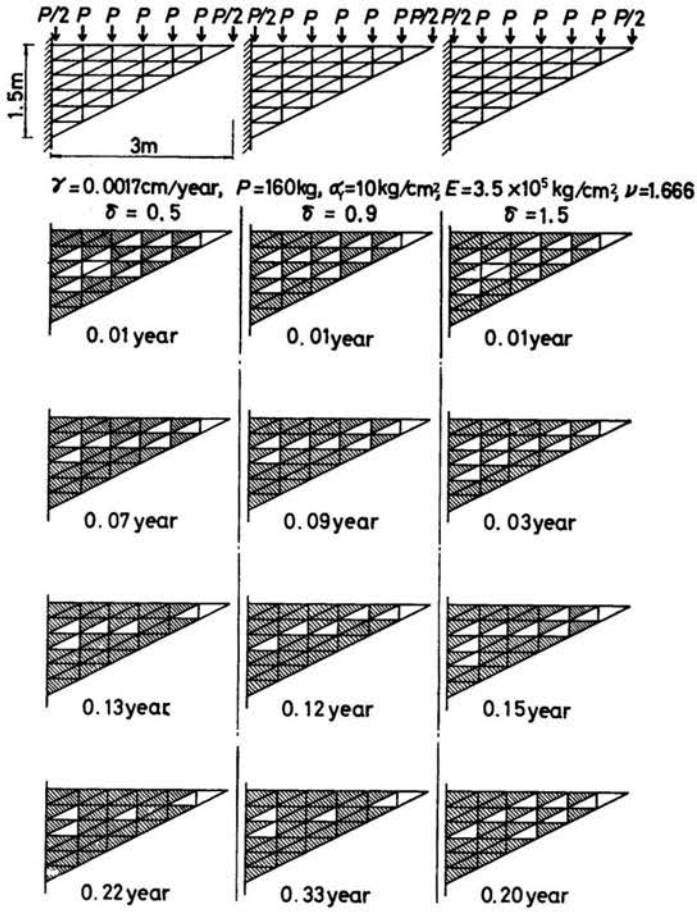


FIG. 10. Yielding regions corresponding to various exponent $\delta$.

The Eqs. (8.9) and (8.11) lead to the constitutive equation for viscoplastic body in the yielding region as follows:

$$S_{ij} = C_{ijkl}\gamma_{kl} + H_{ij}, \tag{8.12}$$

where

$$C_{ijkl} = \lambda^*\delta_{ij}\delta_{kl} + \mu^*(\delta_{ik}\delta_{jl} + \delta_{il}\delta_{jk}),$$

$$\lambda^* = \lambda + \frac{2}{3}(\mu - \mu^*).$$

The following analysis can proceed in the same manner as the conventional finite element method with the use of the Eq. (8.12).

As an illustrative numerical example of elasto viscoplastic body, a cantilever beam with linearly varying cross-section as shown in Figs. 9 and 10 is analyzed under the small strain assumption. Figure 9 is the time stress diagram for the various values of the exponent $\delta$ in the Eq. (8.7). Developments of the plastic region are shown in Fig. 10. It can be understood from the figure that the development of the plastic region is dependent on the values of the exponent $\delta$. Figure 11 illustrates the calculated results of the time

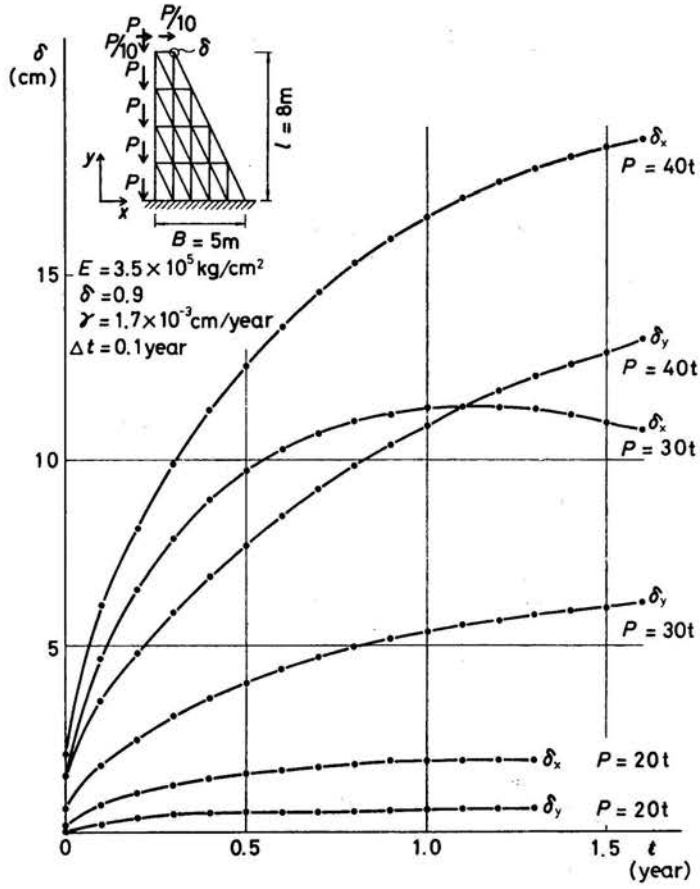


FIG. 11. Time displacement diagram of elasto viscoplastic body.

displacement diagram obtained by the Newton-Raphson procedure using the constitutive equation (8.12) and the finite element formulation of the Eq. (4.11). The calculation was carried out under different values of the external applied load.

## 9. Elastic viscoplastic analysis by the incremental displacement method

Assume that plastic strain rate $\dot{e}_{ij}^{(p)}$ and stress $\tau_{ij}$ are expanded into a power series as:

$$\dot{e}_{ij}^{(p)} = e_{ij}^{(1)(p)}(0) + e_{ij}^{(2)(p)}(0)\Delta t + \frac{1}{2} e_{ij}^{(3)(p)}(0)\Delta t^2 + \ldots, \tag{9.1}$$

$$\tau_{ij} = \tau_{ij}^{(1)}(0) + \tau_{ij}^{(2)}(0)\Delta t + \frac{1}{2}\tau_{ij}^{(3)}(0)\Delta t^2 + \ldots. \tag{9.2}$$

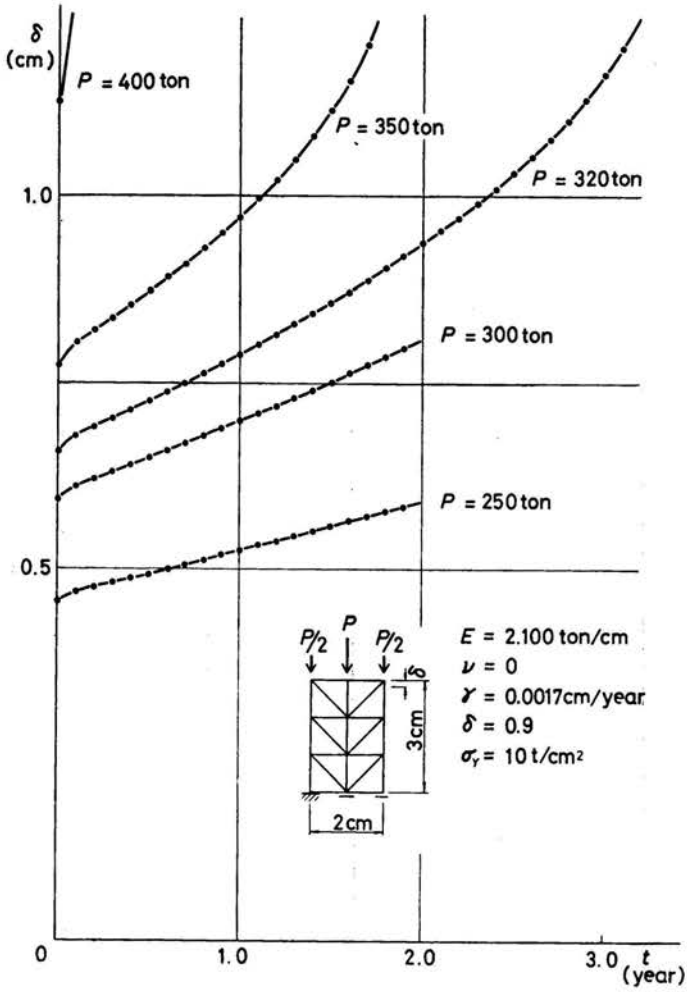


FIG. 12. Time displacement diagram of elasto viscoplastic body.

The Eq. (8.9) with the help of the Eqs. (9.1) and (9.2) yields the following linear simultaneous equation system by comparing the terms of the same order of $\Delta t$ under the assumption that the coefficient $\pi$ in the Eq. (8.9) is constant during short time increment $\Delta t$.

$$
\begin{aligned}
&\pi e_{ij}^{(1)(p)}(0) = \tau_{ij}^{(0)}(0),\\
&\pi e_{ij}^{(2)(p)}(0) = \tau_{ij}^{(1)}(0),\\
&\pi e_{ij}^{(3)(p)}(0) = \tau_{ij}^{(2)}(0).\\
&\cdots\cdots\cdots
\end{aligned}
\tag{9.3}
$$

From the first part of the Eq. (8.9), the relation:

$$S_{ij} = E_{ijkl}\gamma_{kl} - 2\mu\dot{e}_{ij}^{(p)}(0), \tag{9.4}$$

is obtained. In the Eq. (9.4), the elastic modulus $E_{ijkl}$ is used and shown as:

$$E_{ijkl} = \lambda\delta_{ij}\delta_{kl} + \mu(\delta_{ik}\delta_{jl} + \delta_{il}\delta_{jk}). \tag{9.5}$$

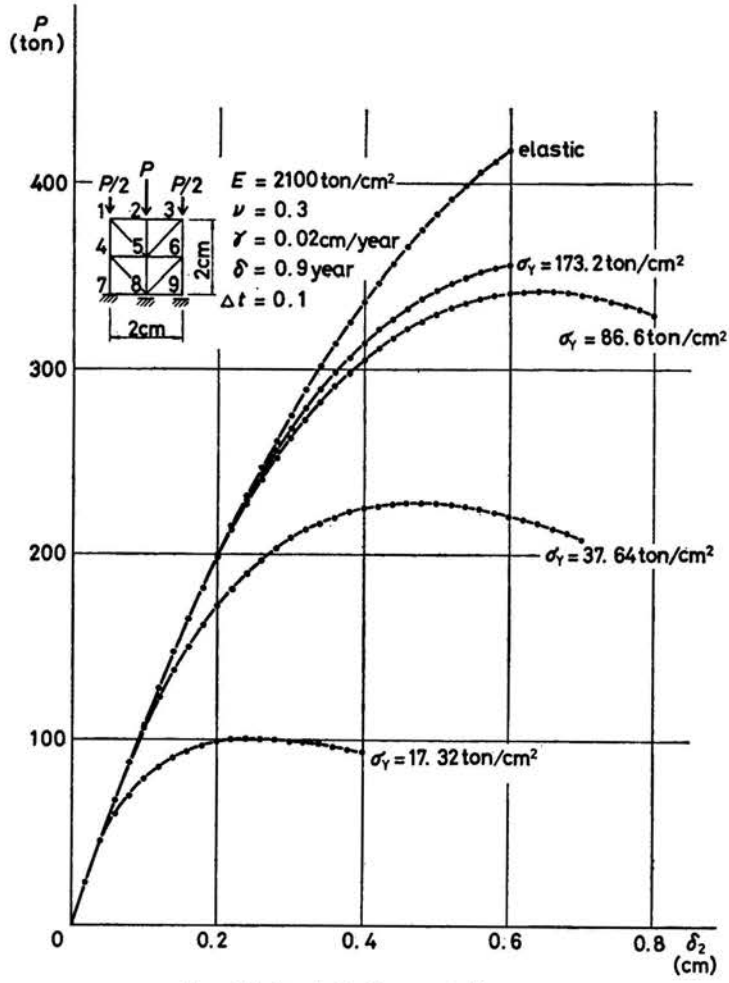


FIG. 13. Load displacement diagram.

Substituting the Eqs. (9.1)–(9.3) into the Eq. (9.4) and rearranging the resulting equation leads to the following equations:

$$
\begin{aligned}
S_{ij}^{(0)}(0) &= E_{ijkl}\gamma_{kl}^{(0)}(0) - 2\mu e_{ij}^{(1)(p)}(0), \\
S_{ij}^{(1)}(0) &= E_{ijkl}\gamma_{kl}^{(1)}(0) - 2\mu e_{ij}^{(2)(p)}(0), \\
S_{ij}^{(2)}(0) &= E_{ijkl}\gamma_{kl}^{(2)}(0) - 2\mu e_{ij}^{(3)(p)}(0), \\
&\cdots\cdots\cdots\cdots\cdots\cdots\cdots\cdots
\end{aligned}
\tag{9.6}
$$

Using the Eq. (9.6), the final governing equation of the finite element method is obtained in the following form:

$$
\begin{aligned}
\bar{K}_{\alpha i \beta j} u_{\beta j}^{(1)} &= \Omega_{\alpha i}^{(1)}(0) + \bar{\Omega}_{\alpha i}^{(1)}, \\
\bar{K}_{\alpha i \beta j} u_{\beta j}^{(2)} &= \Omega_{\alpha i}^{(2)}(0) - \hat{\Omega}_{\alpha i}^{(2)} + \bar{\Omega}_{\alpha i}^{(2)}, \\
&\cdots\cdots\cdots\cdots\cdots\cdots\cdots\cdots
\end{aligned}
\tag{9.7}
$$

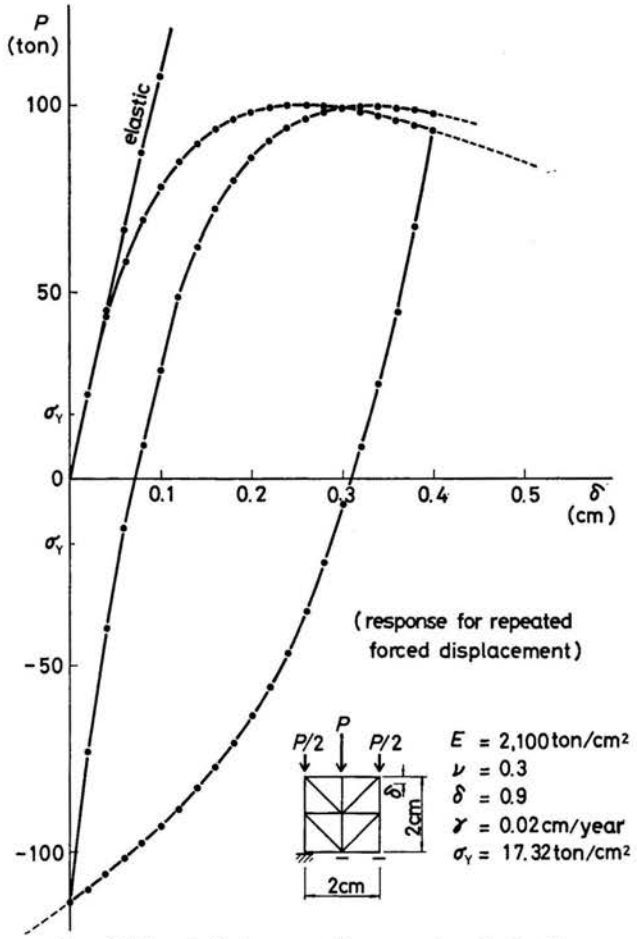


FIG. 14. Load displacement diagram of cyclic loading.

where $\bar{K}_{\alpha i\beta j}$ is the non-linear incremental stiffness matrix as shown in the Eq. (7.15), $\bar{\Omega}_{\alpha i}^{(1)}$ and $\bar{\Omega}_{\alpha i}^{(2)}$ are the equivalent load terms as given below:

$$\bar{\Omega}_{\alpha i}^{(n)} = 2\mu \int_V \Phi_{\alpha,k}\left(\delta_{il}+\Phi_{\gamma,l}u_{\gamma i}(0)\right)e_{kl}^{(n)(p)}dV, \quad n = 1, 2, \tag{9.8}$$

and the equivalent load term $\hat{\Omega}_{\alpha i}^{(2)}$ being the same as in the Eq. (7.16).

Figure 12 shows the calculated time displacement diagram for the different values of the external load $P$. According to the values of the external load, the tertiary creep as well as the secondary creep is calculated in the figure. The load displacement diagram is illustrated in Fig. 13. Calculation was carried out with the different values of yielding stress $\sigma_Y$. Unloading behaviour exceeding the maximum load is calculated in the figure employing the incremental displacement method. For the calculation of cyclic loading behaviour, it is convenient to use the incremental displacement method as shown in Fig. 14. Time stress and the time reaction force diagram are shown in Fig. 15.

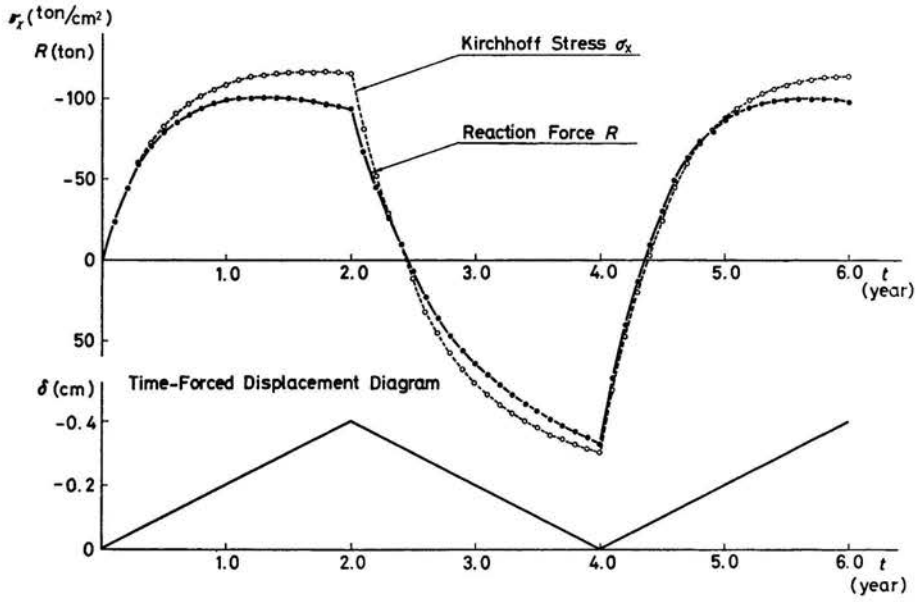


FIG. 15. Time — stress and reaction force diagram.

## 10. Non-linear creep analysis of concrete structure

In the creep analysis of concrete structure, the analysis becomes non-linear since the effect of concrete age should be considered. The constitutive equation for creep behaviour of concrete commonly employs the following equation originally introduced by ARUTYUNYAN:

$$e_{ij} = \frac{\tau_{ij}}{G(t)} - \int_{\tau_1}^{t} \tau_{ij}(s)\frac{\partial}{\partial s}\left[\frac{1}{G(s)}\{1+\varphi(s,t)\}\right]ds, \tag{10.1}$$

$$\gamma_{kk} = \frac{S_{kk}}{K(t)} - \int_{\tau_1}^{t} S_{kk}(s) \frac{\partial}{\partial s}\left[\frac{1}{K(s)}\{1+\varphi(s,t)\}\right] ds, \tag{10.2}$$

where $e_{ij}$ and $\tau_{ij}$ are the deviatoric stress and strain, and $\varphi(s,t)$ is the creep function represented as:

$$\varphi(s,t) = k(s)\varphi_N f(t-s). \tag{10.3}$$

The function $k(s)$ expresses the effect of concrete age, $\varphi_N$ is the creep coefficient of concrete and the function $f(t-s)$ is assumed as:

$$f(t-s) = 1-e^{-\alpha(t-s)}, \tag{10.4}$$

where $\alpha$ is the relaxation constant. The constitutive equation expressed by the Eqs. (10.1) to (10.4) can be transformed into the following incremental form:

$$\ddot{\tau}_{ij} + \dot{\tau}_{ij}\frac{G^{(1)}+G^{(2)}}{C^{(3)}} = G^{(1)}\ddot{e}_{ij} + \frac{G^{(1)}G^{(2)}}{C^{(3)}}\dot{e}_{ij}, \tag{10.5}$$

where

$$G^{(1)} = G(t),$$

$$G^{(2)} = \frac{\alpha G(t)}{\alpha\varphi_N k(t) - \dfrac{\dot{G}(t)}{G(t)}},$$

$$C^{(3)} = \frac{G(t)}{\alpha\varphi_N k(t) - \dfrac{\dot{G}(t)}{G(t)}}.$$

Following the algorithm described in Sec. 3, the Eq. (10.5) is rewritten as:

$$\begin{bmatrix} \dot{\tau}_{ij} \\ 0 \end{bmatrix} = \begin{bmatrix} G^{(1)} & -G^{(1)} \\ -G^{(1)} & G^{(1)}+G^{(2)} \end{bmatrix}\begin{bmatrix} \dot{e}_{ij} \\ \dot{h}_{ij} \end{bmatrix} + \begin{bmatrix} 0 & 0 \\ 0 & C^{(3)} \end{bmatrix}\begin{bmatrix} \ddot{e}_{ij} \\ \ddot{h}_{ij} \end{bmatrix}, \tag{10.6}$$

where $h_{ij}$ is the hidden strain. Since the Eq. (10.6) has a similar relation to the Eq. (3.4), the previously mentioned procedure can be adopted for the Eq. (10.6). Replacing the differentiation with respect to time with the difference with respect to time increment $\Delta t$, the Eq. (10.6) is transformed into:

$$\dot{\tau}_{ij} = \frac{1}{1+\nu}D(t)\dot{\gamma}_{ij} - \frac{1}{1+\nu}\dot{H}_{ij}, \tag{10.7}$$

$$\dot{h}_{ij} = \frac{G^{(1)}}{G^{(1)}+G^{(2)}+\dfrac{C^{(3)}}{\Delta t}}\dot{\gamma}_{ij} + \frac{\dfrac{C^{(3)}}{\Delta t}}{G^{(1)}+G^{(2)}+\dfrac{C^{(3)}}{\Delta t}}\dot{h}(0), \tag{10.8}$$

where

$$\frac{1}{1+\nu}\cdot D(t) = \frac{G^{(1)}G^{(2)}+G^{(1)}C^{(3)}/\Delta t}{G^{(1)}+G^{(2)}+C^{(3)}/\Delta t},$$

$$\frac{1}{1+\nu}\dot{H}_{ij} = \frac{G^{(1)}C^{(3)}/\Delta t}{G^{(1)}+G^{(2)}+C^{(3)}/\Delta t}\dot{h}_{ij}(0).$$

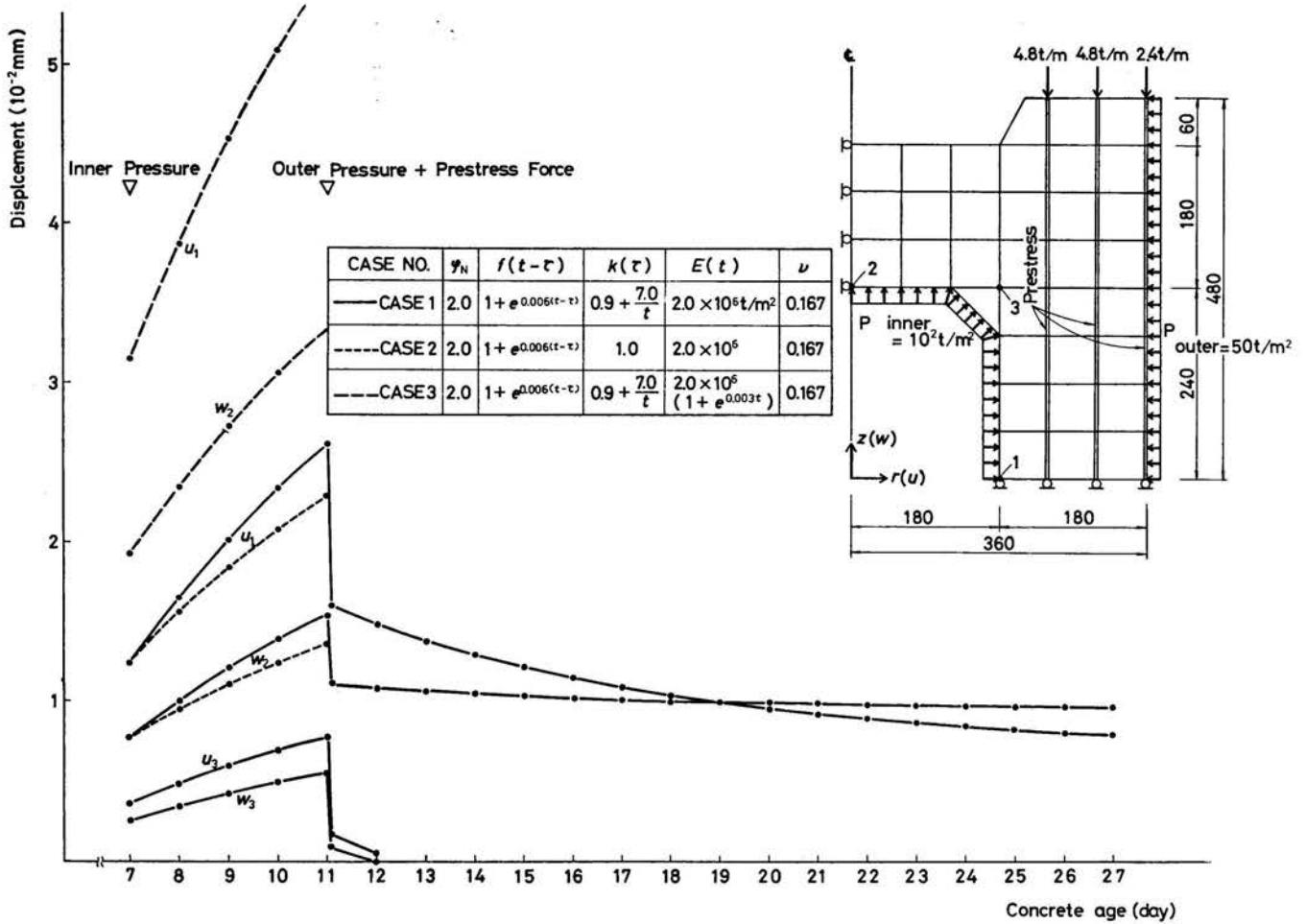


| CASE NO. | $\gamma_N$ | $f(t-\tau)$ | $k(\tau)$ | $E(t)$ | $\nu$ |
|---|---|---|---|---|---|
| ——CASE 1 | 2.0 | $1+e^{0.006(t-\tau)}$ | $0.9+\frac{7.0}{t}$ | $2.0\times10^6$t/m² | 0.167 |
| -----CASE 2 | 2.0 | $1+e^{0.006(t-\tau)}$ | 1.0 | $2.0\times10^5$ | 0.167 |
| ---CASE 3 | 2.0 | $1+e^{0.006(t-\tau)}$ | $0.9+\frac{7.0}{t}$ | $\frac{2.0\times10^5}{(1+e^{0.003t})}$ | 0.167 |

FIG. 16. Creep curve of concrete structure.

For the volumetric components, the same relation is obtained as follows:

$$\dot{S}_{kk} = \frac{1}{1-2\nu} D(t)\dot{\gamma}_{kk} - \frac{1}{1-2\nu}\dot{H}_{kk}. \tag{10.9}$$

Finite element procedure is applicable in the conventional manner using the Eqs. (10.7) and (10.9) as the constitutive equations.

Figure 16 shows the creep curve of axisymmetric concrete structure subject to the internal and external sustained load and prestressed forces as given in the figure under the small strain assumption. Displacements at the nodal points marked 1, 2 and 3 versus concrete age are plotted according to the various constitutive relations. The quadratic shape of finite element with four nodal points was employed in the calculation.

## 11. Conclusion

The present paper has dealt with a finite element method using the constitutive equation expressed by the first-order differential equation related to Green strain, Kirchhoff stress and hidden strain. The replacement of the first-order differential with respect to time $t$ by the difference with respect to the arbitrary short time increment $\Delta t$ led to an equation similar to Hookean elastic body except for the inclusion of the time increment. The procedure was also applied to the study of elasto viscoplastic analysis and certain forms of non-linear creep analysis where all of the non-linear coefficients in the constitutive equation are unchanged during the short time increment. In order to solve discretized non-linear simultaneous equation system, the perturbation method as well as the Newton-Raphson method was employed.

There are two special facts to be noted in the present analysis. The first is the use of the first-order simultaneous differential equation, i.e., the Eq. (3.4) as the constitutive equation. The second is the application of the incremental displacement method to solve large deformation creep and relaxation analysis. The former, namely the use of the first-order simultaneous constitutive equation, is characterized by the following points. It is clear that the Eq. (3.4) corresponds to the rheological model, and the equation can be formulated systematically with the use of the arrays $A^{\mu\lambda}_{,jkl}$ and $B^{\mu\lambda}_{ijkl}$ by the algorithm in the Eq. (3.6). The method is to proceed in steps and the governing equation is formulated as having a similar relation to Hookean elastic body, with corrections to both stiffness coefficients and load terms. The constitutive equation of elasto-viscoplastic body and certain sorts of non-linear creep behaviour can be transformed into an equation having a similar relation to this constitutive equation. The latter, namely the calculation by the incremental displacement method, is marked by the convenience of applying the procedure to highly non-linear problems such as large deformation loading, unloading and cyclic loading behaviours, etc. as illustrated by the numerical examples. The procedure is also applicable to the analysis of relaxation behaviour. The method presented can be adopted for a wide range of rheological analysis of structures and continua.

## 12. Acknowledgement

The writer gratefully acknowledges the Japan Information Processing Service Co., Ltd. for allowing him to use its Burroughs B6700 computer. Part of the numerical examples in this paper were obtained by Mr. Katsumi Kamemura and Mr. Kiyoyuki Okada, research engineers, Taisei Corporation.

## References

1. M. A. BIOT, *Theory of stress-strain relations in anisotropic viscoelasticity and relaxation phenomena*, J. Appl. Phys., **25**, 11, 1954.
2. R. A. SCHAPERY, *Application of thermodynamics to thermomechanical fracture and birefringent phenomena in viscoelastic media*, J. Appl. Phys., **35**, 5, 1964.
3. P. PERZYNA, *The constitutive equations for rate sensitive plastic materials*, Quart. Appl. Math., **20**, 4, 1963.
4. P. PERZYNA, *Thermodynamic theory of viscoplasticity*, Advanc. in Appl. Mech., **11**, 1971.
5. K. HOHENEMSER and W. PRAGER, *Über die Ansatze der Mechanik Isotroper Kontinua*, Z. Angew. Math. Mech., **12**, 216–226, 1932.
6. J. L. WHITE, *Finite elements in linear visco-elasticity*, Proc. 2nd Conf. Matrix Methods Struct. Mech. AFFDL-TR-68-150, Wright-Patterson AFB, 1968.
7. E. B. BECKER and R. E. NICKEL, *Stress wave propagation using extended Rith method*, 10th AIAA Structures, Structural Dynamics and Aeroelasticity Specialist Conference, New Orleans 1969.
8. F. D. S. LYNCH, *A finite element method of viscoelastic stress analysis with application to rolling contact problems*, Int. J. Num. Meth. in Engng., **1**, 4, 1969.
9. D. W. MALONE and J. J. CONNER, *Transient dynamic response of linear visco-elastic structures and continuum*, 10th AIAA Structures, Structural Dynamics and Aero-elasticity Specialist Conference, New Orleans 1969.
10. R. L. TAYLER, K. S. PISTER and G. L. GOUDREAU, *Thermomechanical analysis of visco-elastic solids*, Int. J. Num. Meth. in Engng., **2**, 1, 1970.
11. T. Y. CHANG and Y. R. RASHID, *Viscoelastic response of graphitic materials in irradiation environments*, Nucl. Engng. Desg., **14**, 181–190, 1970.
12. D. W. MALONE and J. J. CONNER, *Finite elements and dynamic viscoelasticity*, J. Engin. Mech. Div., ASCE, **97**, EM4, 1971.
13. T. J. CHUNG and R. L. EIDSON, *Analysis of viscoelastoplastic structural behaviour of anisotropic shells by the finite element method*, 1st. Int. Conf. on Structural Mechanics in Nuclear Technology, Berlin 1971.
14. T. J. CHUNG and R. L. EIDSON, *Viscoelastoplastic response of axisymmetric shells under impulsive loading*, 13th AIAA/ASME/ASHF, Structures, Structural Dynamics, and Material Conference, San Antonio 1972.
15. R. A. ADEY and C. A. BREBBIA, *Efficient method for solution of viscoelastic problems*, J. Engin., Mech. Div. ASCE, **99**, EM6, 1973.
16. O. C. ZIENKIEWICZ, *Finite element method in engineering science*, McGraw-Hill, 1971.
17. J. T. ODEN and G. AGUIRRE-RAMIREZ, *Formulation of general discrete models of thermomechanical behavior of materials with memory*, Int. J. Solids Struct., **6**, 1, 1970.
18. J. T. ODEN, *Finite element formulation of problems of finite deformation and irreversible thermodynamics of nonlinear continua — A survey and extension of recent developments*, R. H. GALLAGHER, Y. YAMADA and J. T. ODEN (eds.), "Recent Advances in Matrix Methods in Structural Analysis and Design", UAH press, 1970.
19. J. T. ODEN, *Finite elements of nonlinear continua*, McGraw Hill, 1972.

20. J. T. ODEN, *Finite element approximation in nonlinear thermoviscoelasticity*, J. T. ODEN and E. R. A. OLIVEIRA (eds.) "Lectures on Finite Element Methods in Continum Mechanics", Lisbon 1971.
21. J. T. ODEN, *Finite element applications in mathematical physics*, J. R. WHITEMEN (ed.), "The Mathematics of Finite Elements and Applications", Academic Press, 1973.
22. J. T. ODEN, D. R. BHANDARI, G. YAGAWA and T. J. CHUNG, *A new approach to the finite element formulation and solution of a class of problems in coupled thermoelasto viscoplasticity of crystalline solids*, Nucl. Engng. Desg., **24**, 1973.
23. M. KAWAHARA and K. HORII, *A numerical analysis on viscoelastic structures by the finite element method*, Proc. J. S. C. E. No. 179, 1970 (In Japanese).
24. M. KAWAHARA and K. HORII, *Large strain, elasticplastic numerical analysis by means of finite element method*, Proc. J. S. C. E., No. 193, 1971.
25. M. KAWAHARA, *Large strain, viscoelastic numerical analysis by means of finite element method*, Proc. J. S. C. E., No. 204, 1972.
26. M. KAWAHARA and K. KAMEMURA, *Elastoviscoplastic finite element analysis by perturbation method*, Finite Element Method in Non-liner Continua, University of Texas, 1974.

DEPARTMENT OF CIVIL ENGINEERING
CHUO UNIVERSITY, TOKYO, JAPAN.